

LANGMUIR PROBE IN ION-BEAM PLASMA: THEORY VS EXPERIMENT**S.V. Dudin***V.N. Karazin Kharkiv National University
Ukraine*

Received 14.09.2012

The paper is devoted to experimental verification of theoretical model of Langmuir probe operation in ion-beam plasma. The mathematical model of single cylindrical Langmuir probe describes dependence of ion current gathered by the probe on the basic parameters of ion-beam plasma. The model covers wide parameters range of the ion-beam plasma, particularly the whole range typical for technological ion-beam systems. The comparison of the results of numerical calculations with the experimental measurement results confirms high reliability of the model in wide range of parameters excluding the case of very low ion beam energy.

Keywords: Langmuir probe, ion-beam plasma, plasma simulation.

Статья посвящена экспериментальной проверке теоретической модели, описывающей работу зонда Ленгмюра ионно-пучковой плазмы. Математическая модель одиночного цилиндрического зонда Ленгмюра описывает зависимость ионного тока на зонд от основных параметров ионно-пучковой плазмы. Модель охватывает широкий спектр параметров ионно-пучковой плазмы, в частности, параметры, типичные для технологических ионно-лучевых систем. Сравнение результатов численных расчетов с экспериментальными результатами подтверждает высокую достоверность этой модели в широком диапазоне параметров за исключением случая очень низкой энергии пучка ионов.

Ключевые слова: зонд Ленгмюра, ионно-пучковая плазма, моделирование плазмы.

Статтю присвячено експериментальній перевірці теоретичної моделі роботи зонда Ленгмюра в іонно-пучковій плазмі. Математична модель одиночного циліндричного зонда Ленгмюра описує залежність іонного струму на зонд від основних параметрів іонно-пучкової плазми. Модель охоплює широкий спектр параметрів іонно-пучкової плазми, зокрема, параметри, що є типовими для технологічних іонно-променевиx систем. Порівняння результатів чисельних розрахунків з експериментальними результатами підтверджує високу достовірність цієї моделі в широкому діапазоні параметрів за винятком випадку дуже низької енергії пучка іонів.

Ключові слова: зонд Ленгмюра, іонно-пучкова плазма, моделювання плазми.

INTRODUCTION

It is known, that in transport space of intense ion beam the ion-beam plasma (IBP) appears as a result of the beam space charge neutralization by electrons [1, 2]. The interest to research of IBP is stimulated by wide extension of different ion-beam technologies [3–6], where the charged, excited, chemically active particles and electromagnetic radiation hit the processed surface immediately from the ion-beam plasma.

One of the most attractive methods for measuring of the ion-beam plasma parameters is the Langmuir probe method, which permit to measure locally practically all essential plasma parameters in wide range of their change. However, the probe measurements in IBP have specific peculiarities connected with complex composition of the plasma, particularly with the presence in the plasma of two ion

groups with dramatically different energies: the beam ions (usually hundreds-thousands eV) and cold plasma ions with temperature much less than 1 eV. Naturally, the response of these two ion groups to the electric field around the probe is different. Slow ion behavior is similar to common plasma, the ions tend to form positive space charge around negatively biased probe while the fast ions don't "feel" the probe voltage and provide constant background of positive space charge with no dependence on the probe voltage.

A mathematical model describing dependence of ion current gathered by single cylindrical Langmuir probe on the basic parameters of ion-beam plasma has been presented in [7]. However, there was no comparison of the simulation results with experiment. The aim of the present work is experimental verification of the theoretical model.

MODEL DESCRIPTION

Let us review first the mathematical model, which describes the dependence of ion current gathered by a single cylindrical Langmuir probe on the basic parameters of ion-beam plasma, such as probe potential, cold and beam ion densities, relation between ion and electron temperatures.

The model is built for collisionless case, because transport of ion-beams takes place at low pressures. A current of cold ions on infinite single cylindrical Langmuir probe is considered. It is assumed that the ion temperature T_i is much less than electrons temperature T_e and electron distribution is Maxwellian. The following dimensionless variables and parameters are used in our model:

$$\psi = \frac{e\phi}{kT_e}, \quad x = \frac{r}{\lambda_{De}}, \quad \eta_i = \frac{n_i}{n_{e0}}, \quad \eta_b = \frac{n_b}{n_{e0}},$$

$$\eta_e = \frac{n_e}{n_{e0}}, \quad x_p = \frac{r_p}{\lambda_{De}}, \quad \psi_p = \frac{e\phi_p}{kT_e},$$

$$i = \frac{I_i}{2\pi r_p L e n_{i0} \sqrt{\frac{2kT_e}{m_i}}}, \quad \tau = \frac{T_i}{T_e}.$$

Here ϕ – potential in point with radius r ; n_p, n_b, n_e – densities of cold ions, beam ions and electrons, respectively; n_{e0}, n_{i0} – densities of electrons and cold ions at infinity, r_p, ϕ_p, L – radius, potential and length of probe; I_i – current of cold ions to the probe; m_i – ion mass; e – electron charge; k – Boltzmann's constant; $\lambda_{De} = \sqrt{\frac{kT_e}{4\pi n_{e0} e^2}}$ – Debye length.

The analogous dimensionless parameters are used in the most of theoretical works dealing with computation of ion current to Langmuir probe [8 – 10], but we have introduced additional parameter: “portion of ion beam in plasma”: $\eta_{i0} = \frac{n_{i0}}{n_{e0}}$. The

value of this parameter changes from 0 (case of “pure” ion-beam plasma without cold ions), to 1 (case of “classic” plasma without beam).

Poisson's equation in dimensionless variables can thus be written as follows:

Poisson's equation in dimensionless variables can thus be written as follows:

Poisson's equation in dimensionless variables can thus be written as follows:

$$\frac{d^2\psi}{dx^2} + \frac{1}{x} \frac{d\psi}{dx} = \exp(\psi) - \left(i\eta_{i0} \frac{x_p}{x} \frac{1}{\sqrt{-\psi}} \right) - (1 - \eta_{i0}),$$

(1)

where the first term of right part is the dimensionless density of electrons, the second is the density of slow ions, the third is the density of beam of ions, which is constant.

For determination of initial conditions let us take a region in which the following conditions are satisfied: $kT_e \gg |e\phi| \gg kT_i, n_e \approx n_i + n_b$. In this region the current density of cold ions can be defined as $j = \frac{I_i}{2\pi r L}$, and on the other hand, the density of cold ions is determined by potential ϕ :

From this equation an analytic expression for radial distribution of potential can be found:

$$j = e n_{i0} \sqrt{\frac{2e(-\phi)}{m_i}}.$$

The initial conditions for equation (1) are set on the cylindrical surface with dimensionless radius x_0 , which is in the region defined above. The potential of this surface we define as $\psi_0 = -b\tau$ where $b > 1$ (for example, $b = 5$). Radius x_0 and derivative of potential at $x = x_0$ can thus be written as follows:

$$\psi(x) = \frac{-i^2 x_p^2}{x^2}.$$

We solved Poisson's equation using the fourth order Runge-Kutta method.

$$x_0 = i x_p \frac{1}{\sqrt{b\tau}}, \quad \left(\frac{d\psi}{dx} \right)_0 = \frac{2b\tau}{x_0}.$$

We solved Poisson's equation using the fourth order Runge-Kutta method.

SIMULATION RESULTS

As a result of numerical computations we have got a data array of cold ion current dependence on four parameters $i(\psi_p, x_p, \eta_{i0}, \tau)$. The values of dimensionless potential were changed from 0 to 50, the dimensionless probe radius x_p from 0.25 to 100 that corresponds to the change of plasma density from 10^8 to 10^{13} cm^{-3} . Temperatures ratio was 0.01. A set of the calculation results is presented graphically in fig. 1.

For the limiting case of the large probe ($x_p = 100$ in the fig. 1) we can make a conclusion, that for any values of parameter η_{i0} , as in the case of “classic” plasma, saturation of ion current takes place. The saturation current density can be presented by formula, which is analogous to the well known Bohm's formula for plasma without ion beam:

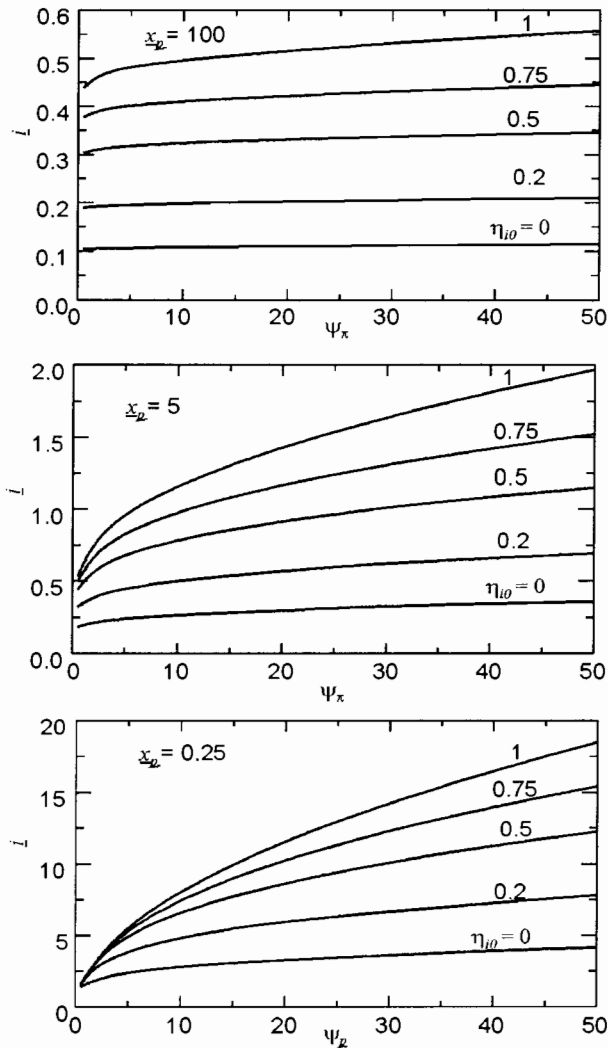


Fig. 1. Evolution of dimensionless ion current to voltage characteristic in dependence on parameter η_{i0} at several x_p values.

$$j = Cen \sqrt{\frac{2kT_e}{m_i}},$$

where coefficient C changes from 0.44 (for plasma without beam), to 0.09 (for ion-beam plasma).

Fig. 2 shows that the ion current depends from η_{i0} almost linearly, and the coefficient C can be presented by formula:

$$C = 0.09 + 0.35\eta_{i0}.$$

For practical usage of numerical results the approximation formula for the current of cold ions on Langmuir probe in ion-beam plasma has been constructed:

$$i = (0.95 + 0.35\eta) \times \left\{ 1 + 1.85(x - 0.05(1 - \eta))^{-3.25/4} \sqrt{40} \left(\frac{\Psi}{40} \right)^{1/2(2-\eta)} \right\}.$$

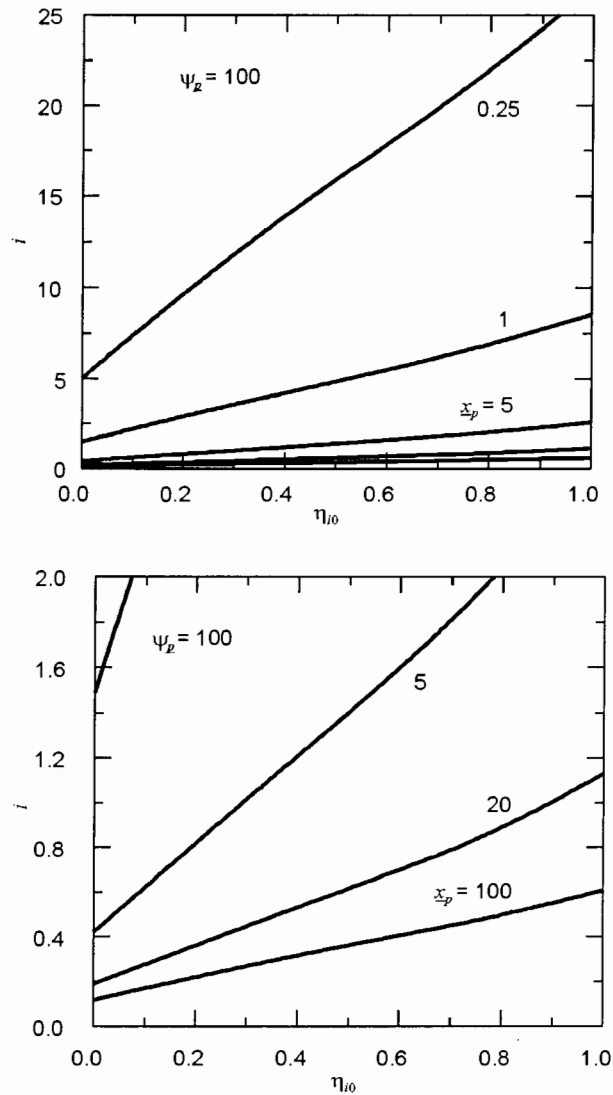


Fig. 2. Ion current i as a function of η_{i0} for the case of high probe potential.

This equation is built in such way that in the limiting case $\eta_{i0} = 1$ the result is equal to classic ABR theory [10]. The difference between the results of this formula and the results of numeral computations is not more 4% in the range of parameters $\psi = 5 - 50$, $\eta_{i0} = 0 - 1$, $x = 0.25 - 100$. For $x > 1$ this equation can be simplified:

$$i = (0.95 + \eta 0.35) \left\{ 1 + 1.85x^{-3.25/4} \sqrt{40} \left(\frac{\Psi}{40} \right)^{1/2(2-\eta)} \right\}.$$

Fig. 3 shows radial distribution of densities of electrons η_e and ions η_i in comparison with potential distribution at several η_{i0} values. One can see that ion density near the probe in IBP is greater, than in “classical” plasma. Therefore, in IBP the sheath is thinner, and the current of cold ions to the Langmuir probe is less than in “classical” plasma with equivalent parameters as has been shown in

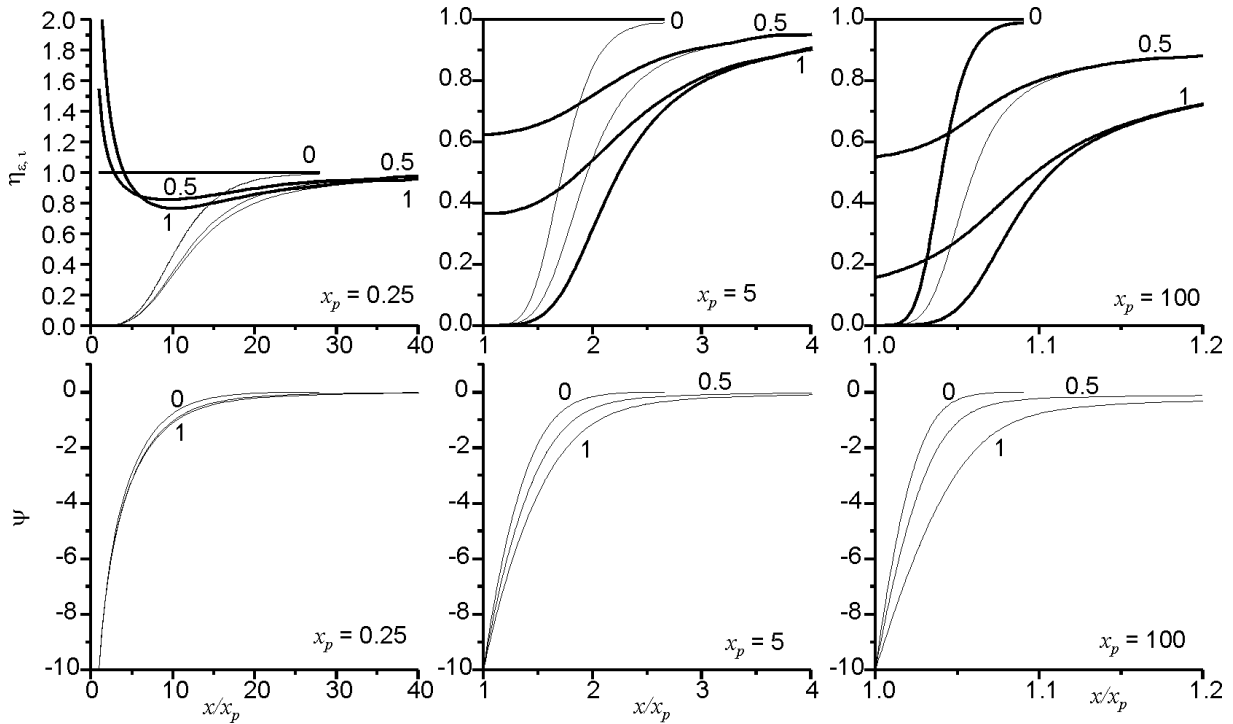


Fig. 3. Radial distribution of densities of electrons η_e and ions η_i in comparison with potential distribution at several η_{i0} values. η_e – thin line, η_i – bold line.

fig. 1.

EXPERIMENTAL TECHNIQUES

In order to provide the experimental verification of the described model in wide range of parameters the experimental investigation was conducted using two different ion sources.

The first experimental setup (Device 1, see fig.4) with a multichannel Hall type ion source “Radical-M” generating ion beam with diameter of about 50 mm, mean ion energy about 500 eV and current 1 – 50 mA. The stainless steel transport chamber with length of 17 cm has approximately rectangular

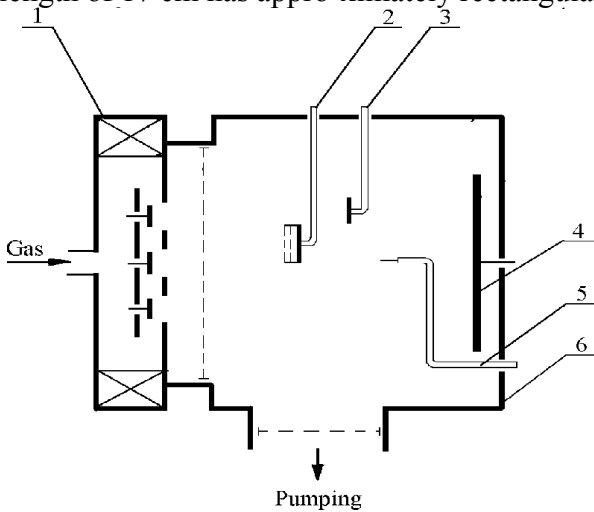


Fig. 4. Scheme of experimental Device 1. 1 – ion source, 2 – multigrad energy analyzer, 3 – flat probe with guard ring, 4 – target, 5 – Langmuir probe, 6 – transport chamber.

cross-section. The argon pressure in the chamber was $10^{-4} - 10^{-3}$ Torr.

The second experimental setup (Device 2, see fig. 5) is based on a single-grid ICP ion source with RF biasing [11]. The plasma is generated by 2-turns shielded inductive coil placed inside the metallic vacuum chamber with 250 mm inner diameter and 80 mm length. RF power (13.56 MHz) in the range 0 – 1000W is applied to the inductor through a matching box. For the control of the plasma potential the discharge chamber was designed as a potential electrode insulated from the grounded flange holding the 0.12 mm thick stainless steel extraction grid with

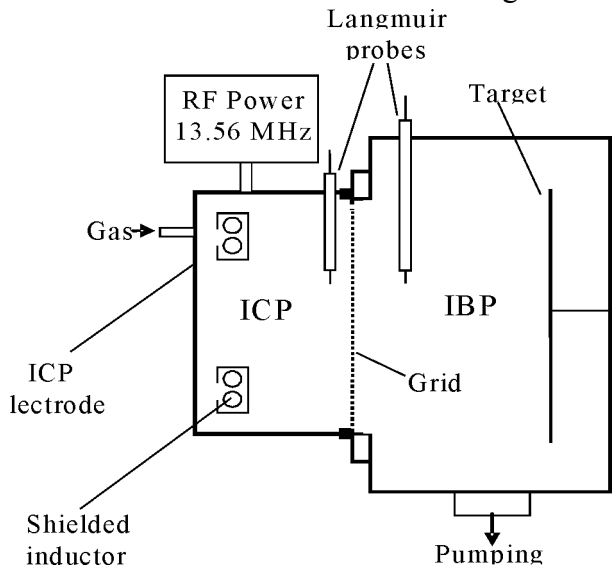


Fig. 5. Scheme of experimental Device 2.

holes of 0.24 mm diameter. The working area of the grid is 450 cm² and optical transparency is 0.4. RF (13.56 MHz) bias voltage required for the ion acceleration is applied between the grounded grid and the source chamber. The RF bias is supplied through a capacitor allowing DC positive self-bias generation on the electrode which is greater than the grid by area. The DC self-bias potential of the electrode was the measured value and is used below as a main parameter governing the ion energy and emission characteristics of the source. All potentials in this work are measured versus the grounded beam transport chamber.

In the described experiments the source was attached to the 400 mm diameter metallic ion beam transport chamber pumped by a turbo pump with 700 l/s throughput. The residual pressure in the system was better than 10⁻⁵ Torr. The 300 mm diameter target accepting the ion beam was placed at 100 mm distance from the source grid. The target was equipped with the 20 mm diameter single-grid retarding-field energy analyzer analogous to the device used in previous works [11 – 13]. The EA grid holes diameter is 0.1 mm, thickness is 0.12 mm and optical transparency is 0.2. Also, a linear array of plane probes biased at -25 V was mounted on the target to measure radial ion current density profile. In order to measure ion current density from the ICP to the IOS an additional planar probe was mounted on the extraction grid at the source axis and also was biased at -25 V.

For measurement of the plasma parameters in both devices Langmuir probes (0.1 mm diameter, 5 mm length) were inserted in the IBP region. The probe measurements were conducted using the PlasmaMeter version 5.3 probe system [14, 15] designed in the V.N. Karazin Kharkiv National University. The current measurement unit and voltage amplifier of the PlasmaMeter are optically isolated from the digital controller connected to ground. PlasmaMeter communicates with the controlling computer via a USB interface. The PlasmaMeter can measure probe currents up to 300 mA at probe voltages from -80 to 80 V. To avoid the probe melting, over-current protection is provided that automatically decreases the probe voltage so that the current drawn through the probe tip never exceeds 0.5 A. Both the ADC and DAC are 16 bits. This in combination with the high linearity of the amplifiers (better than 0.03%), a low internal noise,

and the advanced differentiation procedure used allows measurement of the EEPF to 3 orders of magnitude. The sensitivity is usually limited by plasma noise rather than hardware measurement limitations.

EXPERIMENTAL RESULTS AND DISCUSSION

As it was mentioned in Introduction, the main focus of the present research is to find out the influence of parameters of two groups of ions (namely the fast beam ions and slow plasma ions) on the Langmuir probe trace. The measured current-voltage characteristics of Langmuir probe are shown in fig. 6 for the Device 1 and in fig. 7 for the Device 2.

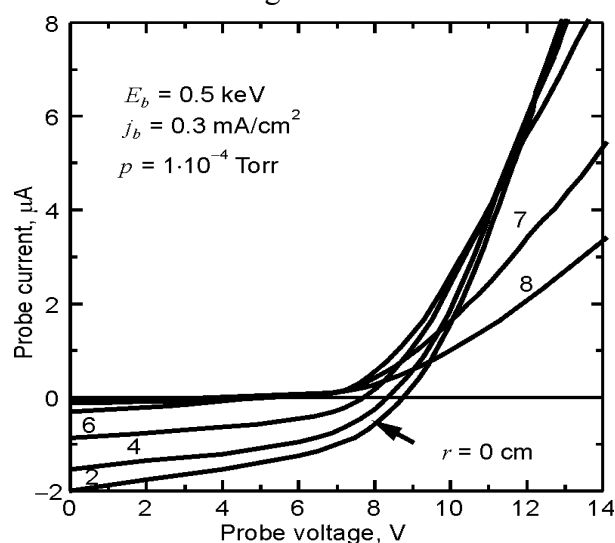


Fig. 6. Langmuir probe characteristics measured in the Device 1. Different curves were measured at different radial probe distances r from the ion beam axis.

The curves in the fig. 6 were measured at the same parameters, but at different probe positions including the positions at the beam axis, at the beam edge and outside the beam, that allows to research the dependence of shape of the probe characteristics on the slow/fast ions ratio with constant ion beam energy.

Otherwise, all the probe curves presented in the fig. 7 are measured at the same probe position (center of the beam transport chamber), but with different ion beam energies in order to reveal the fast ion energy impact on the probe trace. It should be noted that in all the cases the fast ion current to the probe calculated using the known ion beam current density and the probe cross-section area was significantly less than the slow ion current to the probe, so in the comparison of the theoretic and experi-

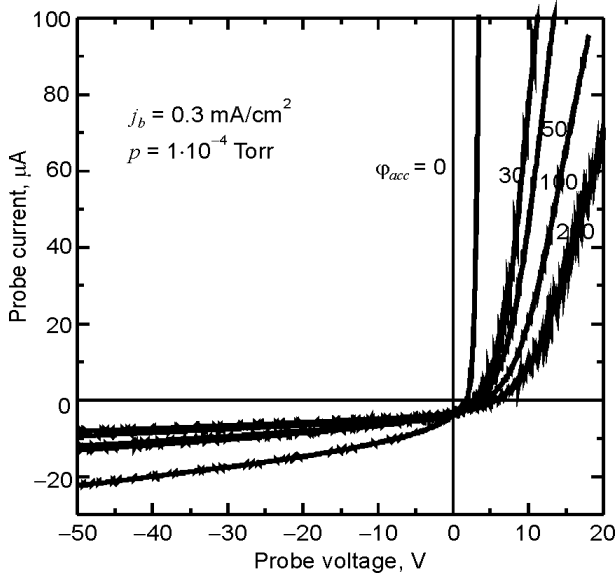


Fig. 7. Langmuir probe characteristics measured in the Device 2. Different curves was measured with different acceleration voltages Φ_{acc} .

mental results below under the ion current to the probe we understand just the cold ion current.

The ion beam energy and current density was measured using the retarding field energy analyzer and the flat probes. Some of the measured ion energy distribution functions are presented in fig. 8. Fast and slow ion peaks are clearly visible. The fast ion peak at high acceleration voltages can be relatively broad, so mean ion beam energy was used in further analysis.

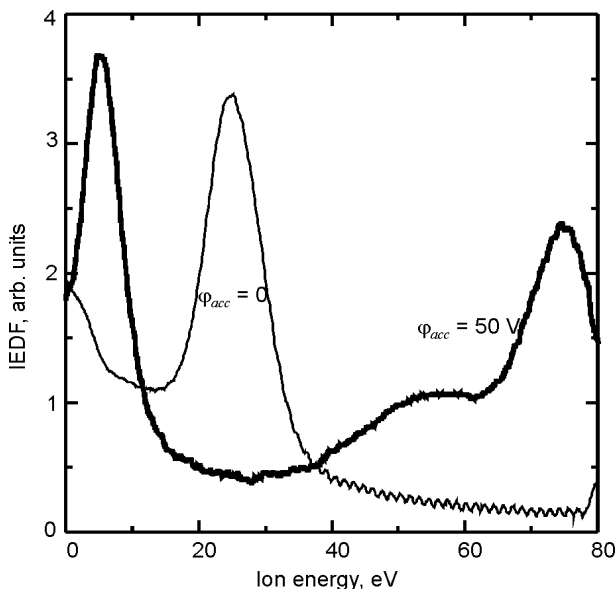


Fig. 8. Measured ion energy distribution functions.

In order to verify reliability of the mathematical model described in the first part of the present paper the direct comparison of the calculated and experimentally measured probe characteristics was

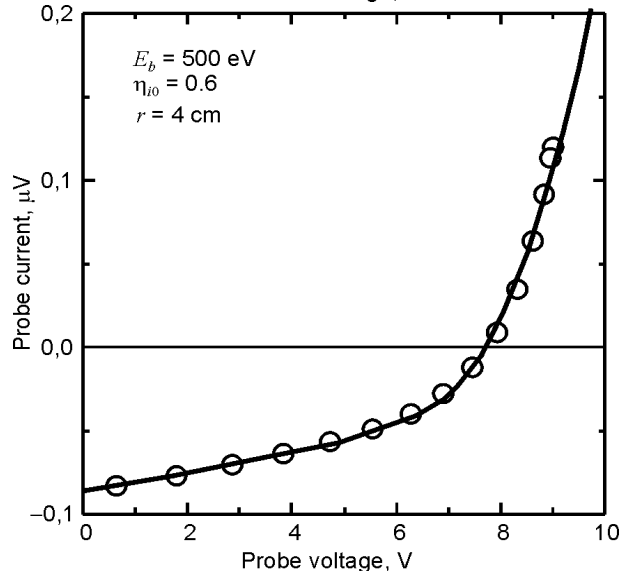
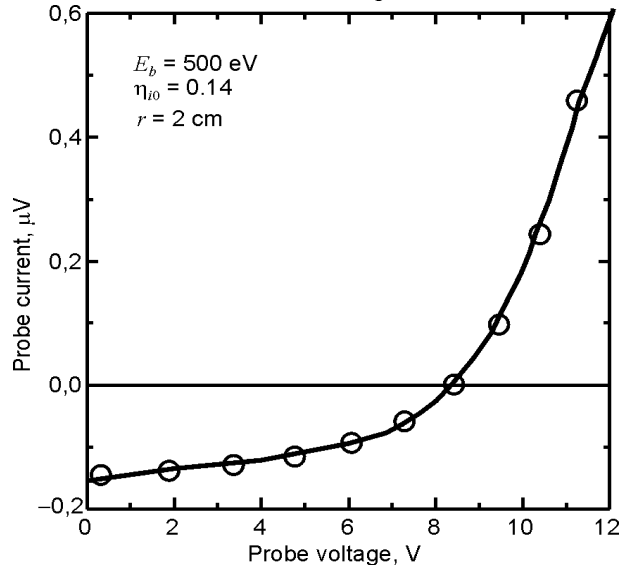
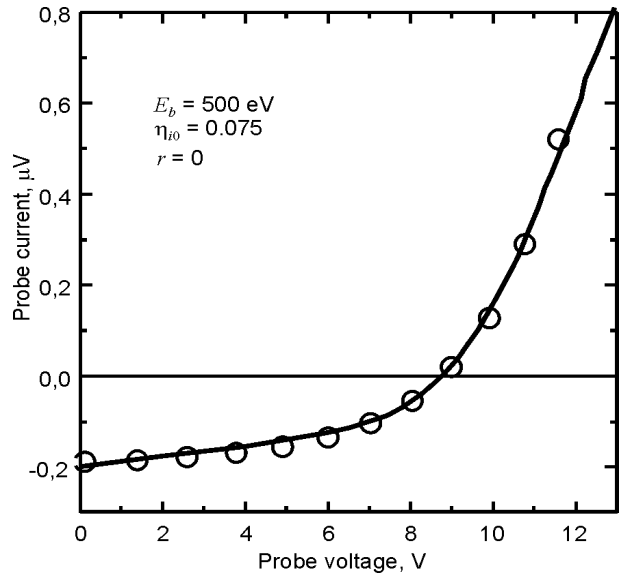


Fig. 9. Comparison of calculated and experimentally measured probe characteristics for Devices 1. Radial probe positions r are the same as in fig.6.

done. Such comparison for the results from the Devices 1 and 2 is illustrated by fig. 9 and 10, re-

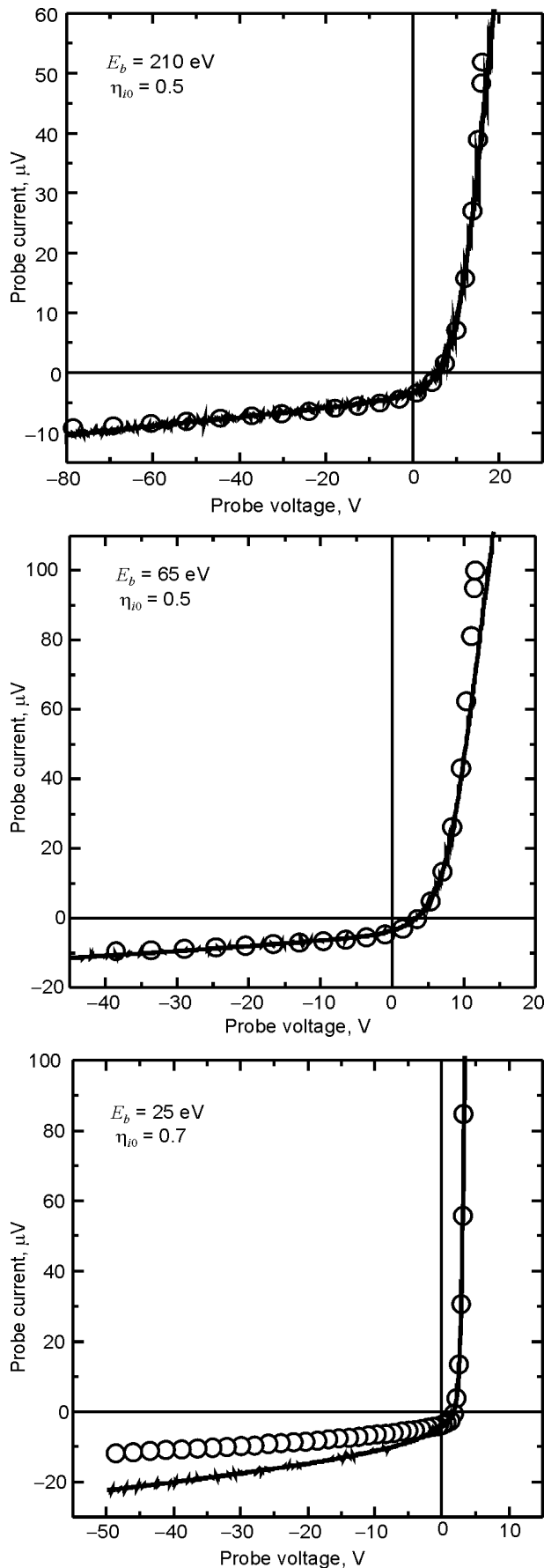


Fig. 10. Comparison of calculated and experimentally measured probe characteristics for Devices 2. Probe is located at the center of the beam transport chamber.

spectively. The calculated dimensionless ion currents were transformed to dimensional form, then electron current calculated using the measured electron temperature was added allowing to obtain complete probe current. The fast ion density was calculated from the measured ion beam energy and current density, slow ion and electron densities was calculated from a guess value of the parameter η_{i0} . Next, using the successive approximation method the right value of η_{i0} was searched for the best coincidence of the theoretic and experimental data.

One can see good agreement of the theory and the experiment for the whole set of parameters excluding the case of very low energy of the ion beam. Presumably it can be explained by the fast ion motion distortion by the electric field around the probe which isn't taken into account by the described model. This looks natural for the lowest ion energies if we compare the probe voltage (up to 50 V in the fig. 10) to the 25 eV ion energy for the last graph in the fig. 10. Thus, we can conclude that the area of applicability of the developed model is limited from the side of low ion beam energy.

Thus, in the present work the experimental verification of the theoretical model of Langmuir probe operation in ion-beam plasma has been carried out. The mathematical model of single cylindrical Langmuir probe describes dependence of ion current gathered by the probe on the basic parameters of ion-beam plasma. The model covers wide parameters range of the ion-beam plasma, particularly the whole range typical for technological ion-beam systems. The results of numerical calculations are presented for the probe current versus probe dimensions and potential as well as the plasma parameters. The analytical expression for the ion current (modification of the Bohm formula) is derived for the large probe limit. For the numerical results the approximation formula is constructed, simplifying practical usage of the results. The comparison of the results of numerical calculations with the experimental measurement results confirms high reliability of the model in wide range of parameters excluding the case of very low ion beam energy.

REFERENCES

1. Gabovich M.D.//UFN.– 1977.– Vol. 121, No. 2. – P. 259-284.
2. Dudin S.V., Zykov A.V., Farenik V.I. Low Energy Intense Ion Beams Space Charge Neutraliza-

- tion//Rev. Sci. Instrum. – 1994. – Vol. 65, No. 4, Part II. – P. 1451-1453.
3. Brown I.G. The Physics and Technology of Ion Sources: Second, Revised and Extended Edition. – Wiley-VCH: New York, 2004.
 4. Reece Roth J., Industrial Plasma Engineering// Applications to Nonthermal Plasma Processing (CRC Press). – 2001. – Vol. 2.
 5. Rius G., Llobet J., Esplandiú M.J., Sole L., Borri-se X., Perez-Murano F.//Microelectronic Engineering. – 2009. – Vol. 86. – P. 892.
 6. Kaufman H.R. Technology of ion beam sources in sputtering//J. Vac. Sci. Technol. – 1979. – Vol. 15, No. 2. – P. 272-276.
 7. Antonova T.N., S Dudin.V., Farenik V.I.//Problems of Atomic Science and Technology. – 2003. – No. 1. – P. 147-149.
 8. Bernstein I.B., Rabinowitz I. Theory of Electrostatic Probes in a Low Density Plasma//Phys. Fluids, 1959. – Vol. 2. – P. 112-115.
 9. Laframboise J. Rarefied Gas Dynamics. Vol. 2/ Ed J.H. de Leeuw, N.Y. – Academic Press, 1966. – 22 p.
 10. Fernandez Palop J.I., Ballesteros J, Colomer V. and Hernandez M.A. Theoretical ion current to cylindrical Langmuir probes for finite ion temperature values//J. Phys. D: Appl. Phys. – 1996. – Vol. 29. – P. 2832-2840.
 11. Dudin S.V., Rafalskyi D.V. and Zykov A.V.//Rev. Sci. Instrum. – 2010. – Vol. 81. – P. 083302.
 12. Dudin S.V. and Rafalskyi D.V.//Europhys. Lett. – 2009. – Vol. 88. – P. 55002.
 13. Rafalskyi D.V. and Dudin S.V.//Appl. Phys. Lett. – 2010. – Vol. 97. – P. 051501.
 14. Dudin S.V.//Devices and technique of experiment. – 1994. – No. 4. – P. 78-82.
 15. McNeely P., Dudin S., Christ-Koch S., Fantz U. //Plasma Sources Sci. Technol. – 2009. – Vol. 18. – P. 014011.